Gene Therapy (2010) 17, 26–36

www.nature.com/gt

ORIGINAL ARTICLE

Suicide gene therapy on spontaneous canine melanoma: correlations between in vivo *tumors and their derived multicell spheroids* in vitro

ML Gil-Cardeza, MS Villaverde, GL Fiszman, NA Altamirano, RA Cwirenbaum, GC Glikin and LME Finocchiaro

[1]*Unidad de Transferencia Genética, Instituto de Oncología 'Ángel H. Roffo', Universidad de Buenos Aires, Buenos Aires, Argentina*

*To validate the use of multicellular spheroids to predict the efficacy of herpes simplex thymidine kinase/ganciclovir (HSV*tk*/GCV) suicide gene therapy in the respective* in vivo *tumors, we established and characterized 15 melanoma-derived cell lines from surgically excised melanoma tumors. Three HSV*tk*-lipofected cell lines were not sensitive to GCV in any culture configuration, other five displayed similar sensitivity as monolayers or spheroids, and only one resulted more sensitive when grown as spheroids. Other six cell lines manifested a relative multicellular resistance (MCR) phenotype growing as spheroids, compared with the same cells growing as monolayers. The reverse correlation between the MCR and the monolayers survival to HSV*tk*/GCV suggests that one of the main causes of MCR would be the rapid cell repopulation after suicide gene treatment. The high correlation of MCR with the spheroids radial growth and with the mitotic index of the respective originary tumors supported this re-growth involvement. A remarkable finding was the high correlation in HSV*tk*/GCV sensitivity between* in vivo *tumor and the corresponding derived cell lines growing as spheroids ($R^2 = 0.85$). This strongly encourages the implementation of spheroids as highly realistic experimental model for optimizing and predicting the* in vivo *response of the respective tumors to therapeutic strategies.*

Gene Therapy (2010) **17,** 26–36; doi:10.1038/gt.2009.107; published online 10 September 2009

Keywords: *spheroids; HSV thymidine kinase; melanoma; lipofection; DMRIE; multicellular resistance*

Introduction

Canine malignant melanoma is a spontaneous tumor displaying histopathological features and biological behavior similar to human melanoma, but a faster progression and an extremely poor prognosis. This highly aggressive canine tumor is too invasive to be cured only by surgical resection and is frequently resistant to current therapies.[1,2] This has prompted investigations to define new treatment strategies. Intratumor suicide non-viral gene therapy with thymidine kinase from the herpes simplex virus (HSV*tk*), in combination with the pro-drug ganciclovir (GCV), is one of the emerging strategies against this malignant disease.[3–5] The successful eradication of tumors depended on the bystander effect,[6] by which unmodified adjacent tumor cells were also destroyed by HSV*tk*/GCV cytotoxic effect, allowing an effective tumor regression produced by only a minority of genetically modified tumor cells.

Malignant melanoma in dogs is also refractory to chemotherapy that may be related to drug resistance manifestation.[1,2] Although this property of tumors was focused for over 20 years on multidrug resistance (MDR), other kind of resistance called multicellular resistance (MCR) produced by a solid tissue environment is the major obstacle to many cancer therapies.[7,8] This intrinsic *in vivo* resistance might not be observed when cells are cultured as monolayers. MCR mechanism is only encountered when cells are cultured as multicellular spheroids (Sphs). These three-dimensional assemblies have been used as experimental models to better reflect the cellular environment that is found *in vivo*.[5–10] Being highly complex systems, their cellular properties are dependent on the origin of the tumor cells, their transformation state, medium and growth conditions. They offer a versatile *in vitro* system of intermediate complexity between monolayer cultures *in vitro* and tumors *in vivo*.[5–10] Sphs combine the relevance of organized tissues with the controlled environment of *in vitro* methodology.[5–10] These cell aggregates organized *in vitro* have a great potential for a number of clinical and biomedical applications. In brief, they represent a more realistic experimental model for optimizing and predicting the efficacy of cancer therapies in the respective *in vivo* tumors.[5–10]

Most of the cancer gene therapy studies carried out on animal models use established tumor cell lines that were kept in culture for many generations, making them very different from the original tumors. We here isolated and characterized 15 canine melanoma cell lines derived from surgically excised melanoma tumors, in order to evaluate potential *in vivo* responses of individual spontaneous canine melanomas to suicide gene therapy.

Correspondence: Dr LME Finocchiaro, Unidad de Transferencia Genética, Instituto de Oncología 'Ángel H. Roffo', Universidad de Buenos Aires, Av. San Martín 5481, 1417 Buenos Aires, Capital Federal, Argentina.
E-mail: gglikin@bg.fcen.uba.ar
Received 18 May 2009; revised 1 July 2009; accepted 1 July 2009; published online 10 September 2009

Table 1 Tumor markers in cultured canine melanoma monolayers

No.	*Cell line*	*Duplication time (h)*	*Vimentin*	*S100*	*Melan A*	*gp100*	*Cytokeratin*
1	Ak	40.4 ± 0.9	+	++	+++	+	–
2	Bk	22.0 ± 2.0	+++	+	+	+	++
3	Br	29.6 ± 0,2	+	+++	+++	++++	++++
4	Btl	45.0 ± 4.1	++++	+++	+++	++	–
5	Bts	35.1 ± 3.0	++++	+	++	–	–
6	Cl	20.8 ± 0.2	+	+	+	+	–
7	Ds	22.2 ± 1.9	+	+	+++	+	–
8	Fk	22.3 ± 2.4	+	+	–	–	–
9	Kg	41.3 ± 2.3	+	++++	++	+	–
10	Ll	21.5 ± 1.7	+	++	–	–	–
11	Rd	43.0 ± 1.1	++++	++	++++	++	+++
12	Rka	28.0 ± 2.0	++++	+	+	+	++
13	Rkb	36.7 ± 0.6	+	+	++	ND	–
14	Sc	25.7 ± 0.3	+	++	++	+	–
15	Tr	22.0 ± 1.0	++++	+	+	–	+

Abbreviation: ND, not determined.
Cells growing for 3 days in monolayers were fixed and treated for markers staining as described in Materials and methods. Time course of growth was determined by trypan blue exclusion cell counting. + symbols indicate semi-quantitative visual estimations: + indicates faint, ++ weak, +++ medium and ++++ strong staining.

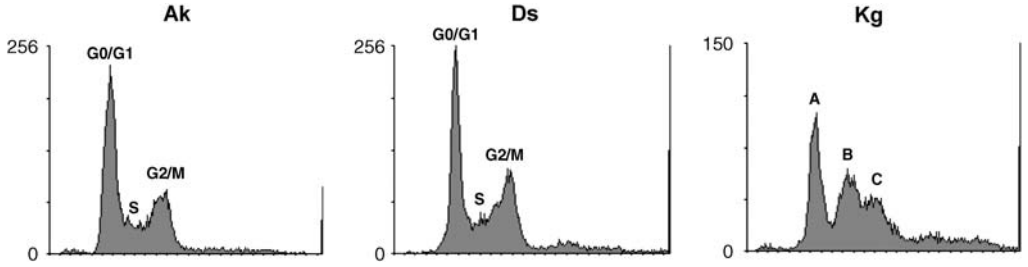

Figure 1 Flow cytometry analysis: cells growing in monolayers for 2 days were suspended, treated and subjected to analysis as described in Materials and methods.

Our results strongly suggest that, the *in vitro* response of tumor-derived Sphs correlated with the clinical outcome of the suicide gene treatment observed on canine melanoma patients *in vivo*. In addition, we present evidence showing that the fast cell repopulation (re-growth) of multicellular Sphs after suicide gene treatment would be mainly responsible for the canine melanoma MCR effect.

Results and discussion

Melanoma derived cell lines displayed considerable heterogeneity

A total of 15 melanoma cell lines, derived from surgically excised hepatic (Ll) and scapular (Bts) metastasis or from oral (Br, Bk, Btl Cl, Ds, Fk, Kg, Rka, Rkb, Rd, Sc and Tr) and ocular (Ak) primary tumors were maintained in culture for over 100 passages.

In accordance with the measured duplication times (DT) of cell lines ranging 20–60 passages, we found three different groups of melanoma cells. A fast group (Bk, Cl, Ds, Fk, Ll, Sc and Tr) displaying a DT $\cong$ 23 h, an intermediate group (Br and Rka) displaying a DT $\cong$ 29 h and a slow group (Ak, Btl, Bts, Kg, Rd and Rkb) displaying DT $\cong$ 40 h (Table 1). Using flow cytometry analysis of DNA content, DTs were confirmed as inversely proportional to the number of cells in S- and G2/M-phases. Two examples are depicted in Figure 1: the highly growing Ds cells, increased the fraction of S-phase cells actively synthesizing DNA and, then, the relative amount of cells in G2/M phase compared with the slow-growing Ak cells.

Cultured as monolayers, 13 cell lines displayed spindle-shaped fibroblastic and 2 epithelioid cell type. Eight of them were faintly adhesive to plastic, as reported for other canine melanoma-derived cell lines,[16] and the remaining ones displayed normal adherence. Kg appeared as three different cell types: (i) fibroblast-like, (ii) large cells with clearly distinguishable nuclei and (iii) giant multinucleated cells (data not shown). The heterogeneity of Kg was indicated by flow cytometry as three peaks (Figure 1). This was probably due to the heterogeneity of the cell cultures as no selection was made to the primary cultures.

Cultured tumor cells expressed melanoma-specific markers

Melanocytes arise from the embryonic neuroectoderm and retain the ability to differentiate into spindled or epithelioid cells, with the identification of canine melanoma being difficult in poorly differentiated amelanotic tumors. Specific markers can help in the diagnosis.

Immunocytochemistry of cells growing as monolayers evidenced uniformly low staining of vimentin (an intermediate filament that is expressed by mesenchymal and neuroectodermal cells in normal tissues) in 9 of 15 cell lines. Conversely Bk, Btl, Bts, Rd, Rka and Tr showed a high vimentin expression. S100, an isoform of a calcium-binding protein restricted to neuroectodermal cells, was high in Br, Btl and Kg; moderate in Ak, Ll, Rd and Sc; and low in Bk, Bts, Cl, Ds, Fk, Rka, Rkb and Tr. Melan A (expressed in pigmented cells) and gp100 (expressed in activated melanocytes) are two specific and sensitive melanoma antigens. Melan A was high in Ak, Br, Btl, Ds and Rd; moderate in Bts, Kg, Rkb and Sc; low in Bk, Cl, Rka and Tr; and negative in amelanotic Fk and Ll. In addition, gp100 staining was high in Br; moderate in Btl and Rd; low in Ak, Bk, Cl, Ds, Kg, Rka and Sc; and negative in Bts, Fk, Ll and Tr. Although a negative staining for cytokeratin (a keratinocyte-specific marker) is expected, five cell lines (Bk, Br, Rd, Rka and Tr) resulted positive. It is noteworthy that these five cytokeratin-positive cell lines also co-expressed vimentin, confirming their invasive and metastatic behavior.[17] Thus, morphological analysis and the positive staining for most of the assayed markers (Table 1) confirmed the diagnosis of melanoma.[18]

Melanoma cells grew in vitro *as multicellular Sphs*

All canine melanoma cell lines were able to grow as multicellular Sphs either in suspension (Figure 2) or as colonies in soft agar (data not shown). Although Br, Btl, Bts, Cl, Ds, Fk, Ll and Rd Sph cells appeared intimately associated with each other and closely packed, Kg, Sc and Tr formed intermediate cell clusters and Ak, Bk, Rka and Rkb appeared as loosely associated aggregates of cells in which single cells could be clearly distinguished (Figure 2, Table 3).

Melanoma Sphs showed considerable response diversity to suicide gene therapy

Multicellular Sphs represent a highly valuable *in vitro* tumor model to explore how the spatial configuration of cells could affect the efficacy of the HSV*tk*/GCV suicide gene therapy under conditions that more closely resemble the *in vivo* situation.[5,10,19] The cytotoxicity of increasing concentrations (0.01–1000 μg ml^{-1}) of the pro-drug GCV was tested on monolayers and Sphs of transiently βgal- or HSV*tk*-expressing melanoma cells.

As shown in Figure 3, sparse growing monolayers derived from different tumors showed very different sensitivities to the HSV*tk*/GCV system. Ak, Bk, Kg, Rka, Rkb and Sc monolayers were the most sensitive with lipofection efficiencies varying from 26–53% (Ak, Bk, Rka and Sc) to 9–12% (Kg and Rkb). On the other hand Br, Fk, and Ll monolayers presenting intermediate lipofection efficiencies (10–17%) and Rd in the low efficiency range (2%) were not sensitive to HSV*tk*/GCV. Conversely, other group with low/intermediate lipofection efficiencies (Btl, Bts, Cl, Ds and Tr: 5–20%) showed intermediate responses to the assayed system. On the other hand, βgal-expressing Ds monolayer cultures showed a higher basal sensitivity to GCV, probably due to high levels of cellular thymidine kinase activity. This precluded evidencing the additional activity of the transferred HSV*tk* gene. Thus, dose–response curves to GCV in βgal- and HSV*tk*-lipofected Ds cells were close.

Although HSV*tk* did not significantly sensitize Br, Fk and Ll cells to GCV in any culture configuration, Ak, Bts, Ds, Rka and Tr resulted similarly sensitive as Sphs or monolayers.

On the other hand, HSV*tk*-lipofected Bk, Btl, Cl, Kg, Rkb and Sc showed Sph cell survival curves that shifted rightward compared with the same cells grown as sparse monolayer, indicating a GCV MCR phenotype when grown as Sphs.

Surprisingly the Sph survival curves of Rd and Tr shifted leftward at the pharmacologically relevant doses of GCV (1–10 μg ml^{-1}) and showed, respectively, moderate and relatively high sensitivity, probably due to a stronger bystander effect in three-dimensional configuration that counteracted the MCR effect.

High lipofection efficiency could explain the efficacy of the HSV*tk*/GCV suicide system in Ak Sphs (53%), in which cell-survival curves were similar to those of the respective sparse monolayers. However, Tr, with intermediate lipofection efficiency (18%), also showed similar monolayer or Sphs cell-survival curves.

Variability in lipofection efficiencies of cell lines could explain the heterogeneity of the responses. Nevertheless, no correlation was observed between monolayers and Sphs survival of the sensitive group and their lipofection efficiencies (data not shown).

As shown in Table 2, Sphs/monolayers IC_{50}s evidenced that Sphs sensitivity to suicide gene treatment was quantitatively different for each individual tumor and independent of the respective monolayers response. HSV*tk*-expressing Bk, Btl, Cl, Kg, Rkb and Sc Sphs resulted hardly sensitive, whereas Bts, Ds and Rka only moderately sensitive to GCV compared with their respective monolayers. In assays carried out in three-dimensional cultures, HSV*tk*-lipofected Ak, Ds, Rd, Rka, Rkb, Sc and Tr cells were 3- to 1064-fold more sensitive to GCV than the corresponding βgal-lipofected controls, supporting the feasibility of this suicide approach *in vivo*. Conversely, HSV*tk*-lipofected Fk, Kg and Ll Sphs did not show any significant increased sensitivity to GCV with respect to the corresponding βgal-lipofected cells. Bk, Br, Btl, Bts and Cl showed survival values higher than 100% at the lower concentrations of GCV. Although the HSV*tk* survival curves were always below the βgal ones, their high survival values ($>50\%$) precluded the determination of IC_{50}s for both.

Suicide gene cytotoxicity at an in vivo *significant intratumor GCV concentration*

We estimated the HSV*tk* suicide gene cytotoxicity at the pharmacologically relevant GCV concentration of 1 μg ml^{-1}, similar to an intratumor standard dose of our canine patients.[3,4] Under this condition, that more closely resemble the *in vivo* situation, the suicide gene killed a substantial amount of sensitive HSV*tk*-expressing cells, with little effect on βgal-expressing cells (Figure 3).

When grown as sparse monolayers, 4 of 15 cell lines appeared not to be sensitive to the HSV*tk*/GCV (1 μg ml^{-1}) system (Figure 4a), whereas the remaining 11 cell lines showed survival values significantly lower than β-gal lipofected controls (Figure 4b, c). Three of four cell lines whose monolayers were not affected by the suicide system maintained the non-responsiveness when

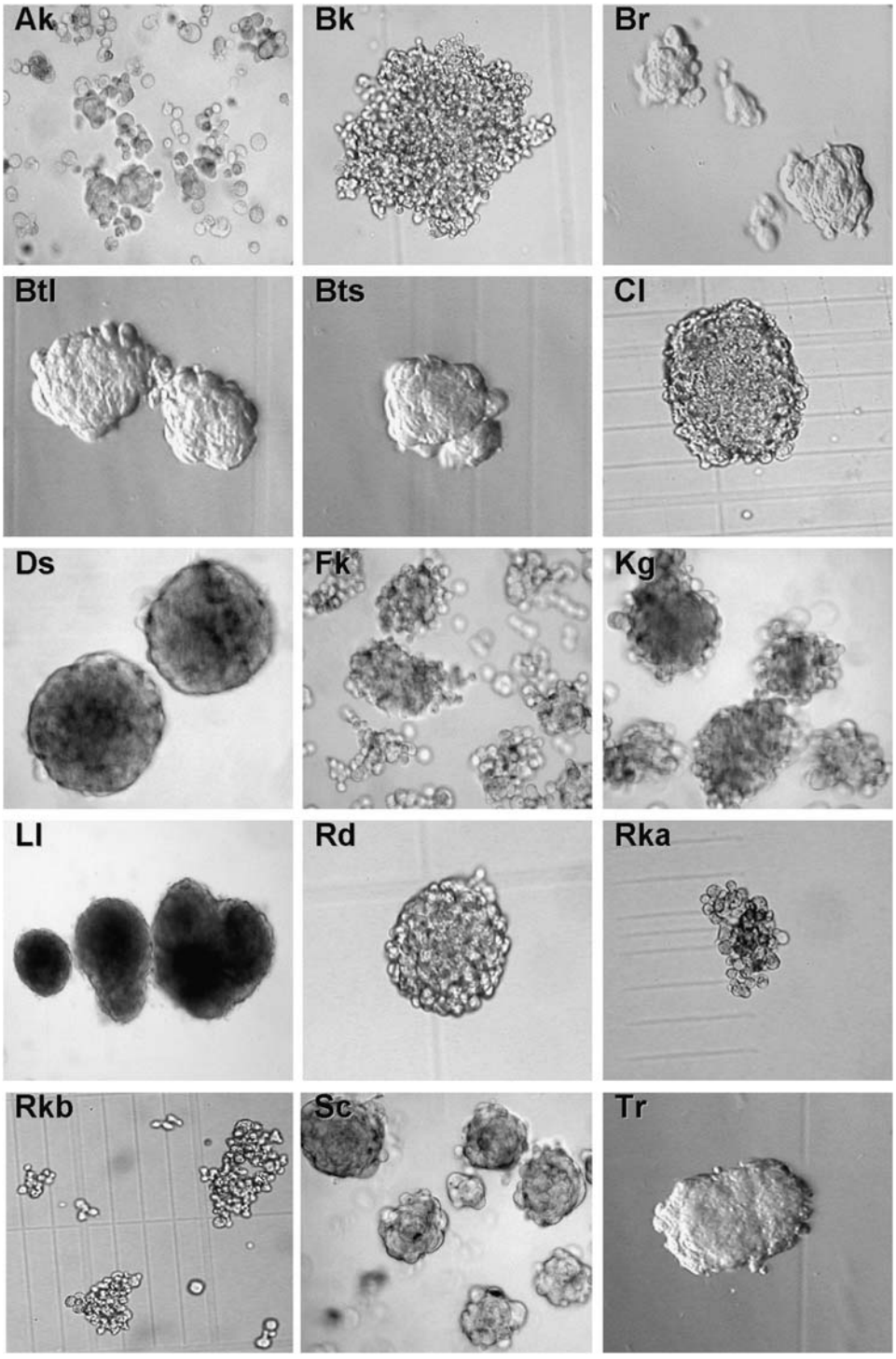

Figure 2 Canine melanoma spheroids morphology: canine melanoma-derived cells growing in suspension for 3 days were observed by a inverted phase contrast microscope and photographed ($\times 200$).

grown as Sphs. Only Rd Sphs, whose monolayers were nonsensitive to HSV*tk*/GCV, were significantly inhibited by this suicide system ($P<0.001$). In the susceptible monolayers (Mnl) group (11 cell lines), 7 cell lines (Ak, Bk, Bts, Ds, Rka, Rkb and Tr) maintained a significant response to HSV*tk*/GCV when grown as Sphs, whereas the remaining 4, lost their responses (Btl, Cl, Kg and Sc).

Only 6 of 11 cell lines (Bk, Btl, Cl, Kg, Rkb and Sc) presented MCR phenotype: (%Mnl survival values significantly lower than %Sph), whereas the remaining 5 (Ak, Bts, Ds, Rka and Tr) did not. Nevertheless, two of six MCR-positive and five of five MCR-negative Sphs showed a survival rate significantly lower than the βgal-expressing Sphs. These results suggest that, despite the MCR effect, the HSVtk/GCV system is sufficiently effective to be successfully applied to melanoma cells both *in vitro* and *in vivo* in about 50% of the cases.

In vitro *suicide gene resistance of Sphs inversely correlated with the monolayers' sensitivity*

To quantify the effect of the spatial configuration on the action of the suicide system we calculated a MCR index (MCRi) as follows: MCRi = (%Sph—%Mnl)/%Mnl. As shown in Figure 5, we found a reverse correlation between the MCRi and the percentage of survival of the monolayers, apparently following a potential tendency ($R^2 = 0.81$).

Suicide gene sensitivity of Sphs correlated with the in vivo *tumor response of canine melanoma patients*

As it was already reported,[3,4] spontaneous melanoma canine patients received 5-weekly intratumor injections

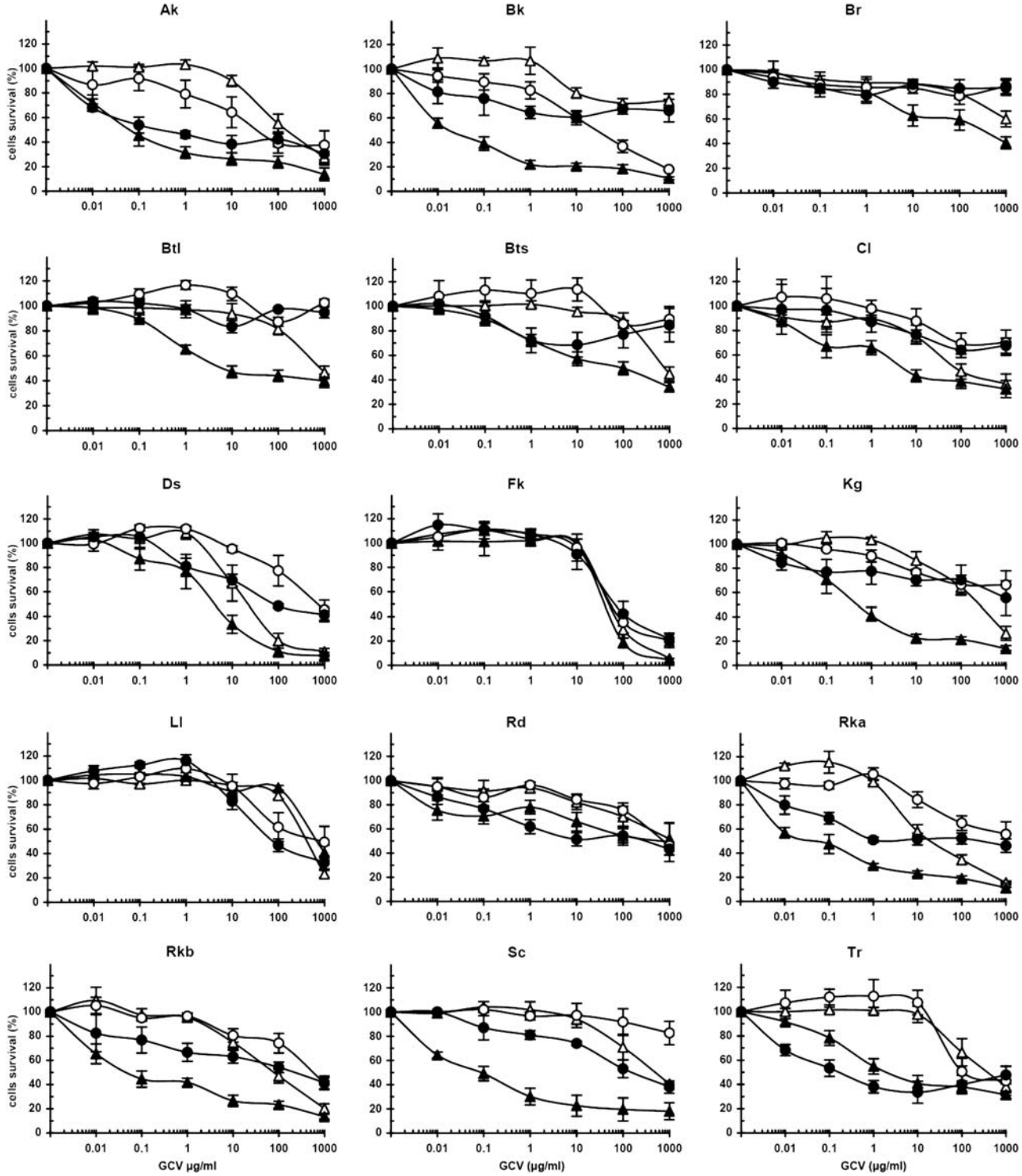

Figure 3 *In vitro* HSV*tk*/GCV effects on monolayers and spheroids: *In vitro* GCV dose–response curves of canine melanoma-derived βgal (○, △)- and HSV*tk*- (▲, ●)-expressing cells growing as monolayers (△, ▲) or spheroids (○, ●). The assay was performed as described in Materials and Methods. Results were expressed as mean ± s.e.m. of four independent experiments.

Table 2 *In vitro* sensitivity to GCV of HSV*tk*- and βgal-expressing multicellular spheroids and monolayer cultures

Cell line	*Monolayers*		*Spheroids*		*βgal/HSVtk*		*HSVtk: Spheroid/ Monolayer*	*Lipofection efficiency (%)*
	βgal	*HSV*tk	*βgal*	*HSV*tk	*Monolayer*	*Spheroid*		
Ak	230 ± 78	0.27 ± 0.19	34 ± 17	0.82 ± 0.22	849	41	3	53 ± 14
Bk	12 ± 7	0.025 ± 0.01	>1000	>1000	474	>1	>40500	43 ± 8
Br	>1000	297 ± 144	>1000	>1000	3.4	>1	>3.4	10 ± 1
Bts	760 ± 163	105 ± 74	>1000	>1000	7.3	>1	>9,6	11 ± 3
Btl	750 ± 166	6.8 ± 1.5	>1000	>1000	110	>1	>146	5 ± 2
Cl	79 ± 50	5.0 ± 2.0	>1000	>1000	15	>1	186	20 ± 4
Ds	30 ± 10	3.0 ± 2.0	390 ± 132	77 ± 15	10	5	25	9 ± 5
Fk	68 ± 23	39 ± 3.0	56 ± 19	67 ± 21	1.7	0.8	2	10 ± 3
Kg	309 ± 131	0.64 ± 0.45	>1000	>1000	483	>1	>1500	9 ± 4
Ll	470 ± 58	477 ± 62	64 ± 26	159 ± 114	1	0.4	0.3	17 ± 8
Rd	336 ± 212	202 ± 117	730 ± 76	30 ± 5	1.7	24	0.15	2 ± 1
Rka	24 ± 16	0.05 ± 0.02	>1000	0.94 ± 0.04	474	>1064	19	32 ± 9
Rkb	76 ± 32	0.045 ± 0.01	578 ± 153	205 ± 81	1690	2.8	4550	12 ± 1
Sc	392 ± 123	0.14 ± 0.05	>1000	133 ± 68	2798	>8	946	26 ± 11
Tr	354 ± 110	2.6 ± 1.2	108 ± 32	0.17 ± 0.09	135	650	0,06	18 ± 3

Abbreviations: GCV, ganciclovir; HSV*tk*, herpes simplex thymidine kinase.
Lipofection efficiency was measured as blue X-Gal-stained cells. The results represent means s.e.m. of (4) independent experiments of GCV concentrations leading to 50% reduction in cell viability (IC50) from the experiments showed in Figure 3.

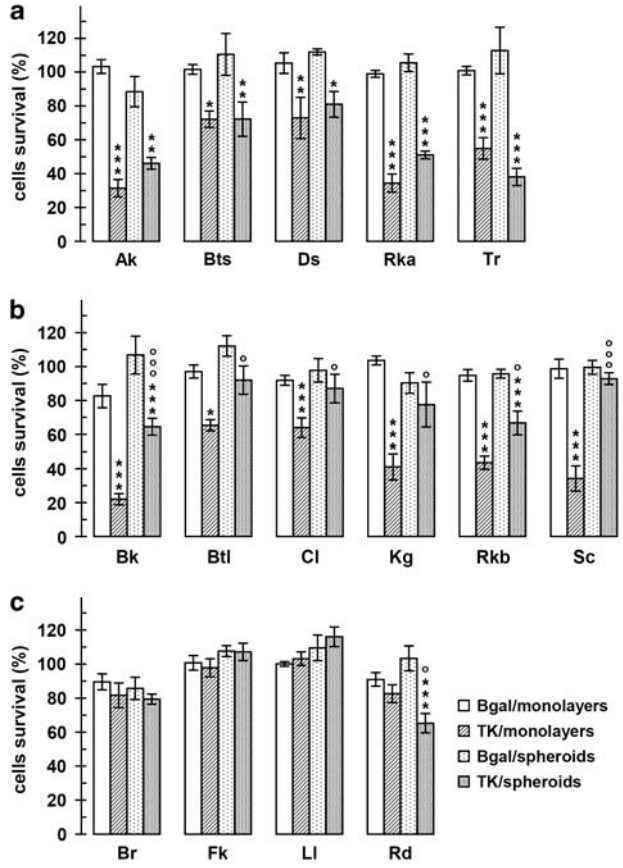

Figure 4 *In vitro* sensitivity to 1 μg ml^{-1} GCV of HSV*tk*- and βgal-expressing multicellular spheroids or monolayer cultures. The results represent means ± s.e.m. of four independent experiments at 1 μg ml^{-1} GCV concentration derived from Figure 3. In this case, each value was relative to the respective condition in the absence of GCV. (**a**) Cells not displaying MCR; (**b**) cells displaying MCR; and (**c**) monolayers not sensitive to the HSV*tk*/GCV system. HSV*tk* vs βgal: ***$P<0.001$; **$P<0.01$; *$P<0.05$. Spheroids vs monolayers: °°°$P<0.001$; °$P<0.05$.

of HSV*tk*-carrying lipoplexes and GCV. Table 3 summarizes the suicide gene therapy responses of *in vivo* tumors and the respective derived cell lines growing as monolayers and Sphs.

Among the six tumors (Btl, Bts, Br, Cl, Ds and Sc) that showed stable disease (s.d.) during the 5 weeks of suicide gene treatment (Table 3), five (except Bts) maintained their non-response to HSV*tk*/GCV when grown as Sphs, whereas five of six (except Br) were sensitive to suicide gene lipofection when grown as monolayers (Figure 4). Among the seven tumors that showed objective responses (Ak, Bk, Kg, Rd, Rka, Rkb and Tr), six maintained their significant response to HSV*tk*/GCV when grown as Sphs, whereas Kg lost it. Although grown as monolayers, six of seven cell lines (except Rd) remained sensitive to HSV*tk*/GCV (Table 3).

A remarkable finding was the high correlation in HSV*tk*/GCV sensitivity between *in vivo* tumors and the corresponding derived cell lines when grown as Sphs ($R^2=0.85$). This result became more significant as no correlation was found with the same transiently lipofected cells cultured as sparse monolayers ($R^2=0.29$) (Figure 6).

This correlation between the *in vitro* behavior of Sphs and the clinical outcome of the HSV*tk*/GCV treatment on canine melanoma patients *in vivo* (Figure 6) strongly encourages the implementation of Sphs as a highly realistic experimental model for optimizing and predicting the *in vivo* response of the respective tumors to therapeutic strategies.

In addition, these data suggest that the MCR to suicide gene treatment found in Sphs also occurred in the tumors *in vivo*.

One limitation of cultured Sphs in terms of emulating the tumor microenvironment is the fact that they do not contain stromal cells, such as fibroblasts, endothelial cells and immune cells including macrophages, NK, T/B lymphocytes, etc. Although we can assume that stromal cells would have a key role *in vivo* for the long-term

outcome of a treatment, in this particular case, it seems that the HSV*tk*/GCV treatment on Sphs, mainly composed by polyclonal tumor cells, constituted a very good model mimicking the *in vivo* situation. This suicide gene system could rely mainly on the direct effect on the tumor cells. Chopped tumor slices, a model of a limited amount of tumor containing the whole stromal structure, showed similar HSV*tk*/GCV response to those obtained with the respective Sphs (data not shown). In addition, canine melanomas usually presented low infiltration of immune cells, and the increase of this infiltration after treatment with suicide gene with respect to pretreatment biopsies was not sufficient to break the immune tolerance to self-antigens and the immunosuppressive tumor microenvironment.[3] Therefore, the effectiveness of HSV*tk*/GCV bystander effect may not be restricted to the immune cell infiltration response, but specially to mitochondria amplification of HSV*tk*/GCV-induced apoptosis/necrosis. Mitochondrial free radicals, diffusing or passing to adjacent cells leading them to oxidative damage, would allow that only few HSV*tk*-expressing cells could initiate the destruction of almost the whole Sph.[10]

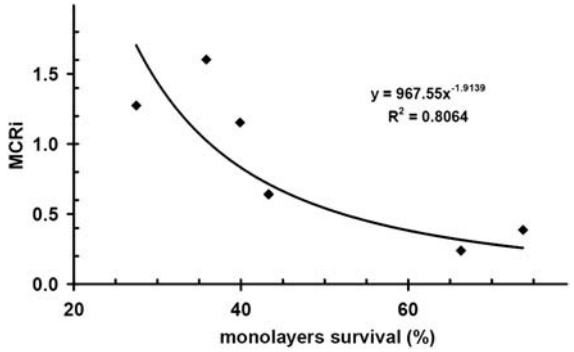

Figure 5 Spheroid multicellular resistance index (MCRi): Correlation at 1 μg ml^{-1} GCV with respect to the survival of the corresponding the monolayer. Each dot corresponds to an individual experiment. Only cell lines displaying MCR were included in the plot. Tendency curves were calculated by potential regression.

In vivo *and* in vitro *tumor cell suicide gene resistance could be due to 're-growth resistance'*

The replication active part of Sphs, sensitive to the suicide system, mainly belongs to the outer layers of Sphs, as monolayers on the surface of a sphere.[10,15] Then, it could be inferred that the inverse correlation between Sphs MCR and monolayers survival would be due to a faster repopulation, through recruitment of the surviving quiescent cells to the proliferative fraction after suicide gene treatment.[10,15,20] If this were the case, the MCRi should correlate with the rate of Sph radial growth. This was, in fact, observed (as shown in Figure 7a), because the daily radial increase of Sphs during the linear phase of growth was proportional to that of the MCRi, following a linear tendency ($R^2 = 0.98$). Conversely, no correlation was found between the monolayers DT and the MCRi ($R^2 = 0.126$) or the daily Sphs radial increase ($R^2 = 0.303$) (plots not shown). Furthermore, we did not find any correlation between MCRi and the degree of compactness of Sphs, parameter that can modify non-viral transgene expression.[15]

The phenomenon, termed 're-growth resistance,' has already been showed in patients and it was found also in Sphs.[20–21] After radiotherapy or chemotherapy, a great proportion of well-oxygenated external cycling cells die. Subsequently, quiescent cells that become situated at the periphery of the Sphs have better access to nutrients. These quiescent cells thus return to the cell cycle, resume growth and the new cells take the vacant places in the tumor.

Table 3 Melanoma responses to suicide gene transfer

Patient/cell line	In vivo				In vitro		
	Tumor mitotic index	*Tumor volumes*		*Clinical Response*	*Survival (%)*		*Spheroids Compactness*
		Initial (cm³)	*Final (%)*		*Monolayers*	*Spheroids*	
Ak	2.5 ± 0.3	1 ± 0.2	25 ± 3	PR	31 ± 5	46 ± 3	+
Bk	3.3 ± 0.7	15 ± 2	49 ± 5	PR	22 ± 3	64 ± 5	+
Br	4.2 ± 0.5	4 ± 0.4	70 ± 8	s.d.	87 ± 7	79 ± 3	+++
Btl	4.0 ± 0.6	25 ± 3	123 ± 14	s.d.	65 ± 3	97 ± 8	+++
Bts	2.5 ± 0.3	87 ± 9	59 ± 7	s.d.	72 ± 5	72 ± 10	+++
Cl	2.0 ± 0.4	36 ± 5	85 ± 9	s.d.	66 ± 6	87 ± 8	+++
Ds	4.1 ± 0.5	17 ± 2,3	65 ± 8	s.d.	73 ± 12	81 ± 8	+++
Fk	4.5 ± 0.7	12 ± 2	>600	PD	98 ± 5	107 ± 5	+++
Kg	3.5 ± 0.4	3 ± 1	50 ± 7	PR	41 ± 8	78 ± 13	++
Ll	4.5 ± 0.6	13 ± 1.4	>345 n.t.	PD	103 ± 4	116 ± 6	+++
Rd	3.9 ± 0.5	25 ± 3.5	48 ± 6	PR	78 ± 5	62 ± 6	+++
Rka	3.2 ± 0.4	20 ± 2.4	43 ± 5	PR	30 ± 4	51 ± 2	+
Rkb	3.0 ± 0.3	55 ± 7.8	48 ± 7	PR	42 ± 5	67 ± 7	+
Sc	4.0 ± 0.4	12 ± 1.5	62 ± 8	s.d.	34 ± 7	84 ± 3	++
Tr	2.2 ± 0.2	22 ± 3.2	35 ± 5	PR	55 ± 6	38 ± 5	++

Abbreviations: n.t., not treated; PD, progressive disease; PR, partial response; s.d., stable disease.
Canine patients were treated and tumor volumes were measured at day 42 as described.[4] Monolayers and spheroids survivals correspond to 1 μg ml^{-1} GCV pro-drug concentration (see Figure 3).
Tumor mitotic index was the average number of mitotic figures counted in 10 consecutive, non-overlapping high-power fields (500 μm in diameter). + symbols are used for the degree of compactness as seen in Figure 2.

As expected, MCRi also correlated with the mitotic index of the original tumors ($R^2 = 0.93$), strongly supporting the theory of fast repopulation by cell re-growth as responsible of the MCR (Figure 7b). These results, in agreement with already reported data showing that the mitotic index highly correlated with malignancy,[22] would explain the extremely fast *in situ* progression of these highly aggressive tumors in the patients.[4]

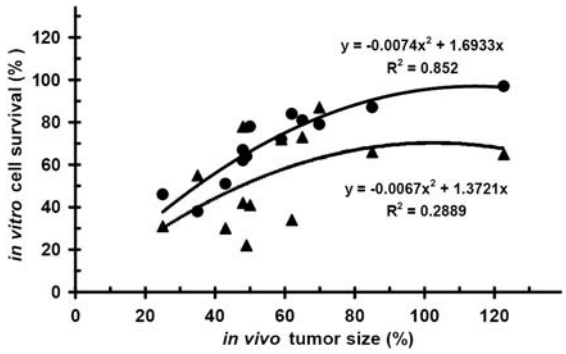

Figure 6 *In vitro* vs *in vivo* sensitivity to the suicide gene system: Correlation of the *in vitro* cell survival with suicide gene/GCV (1 μg ml^{-1}) in monolayers (▲) and spheroids (●) at day 5 and 12, respectively (Figure 4), and the *in vivo* original tumor responses after 5-weekly treatments (Table 3). Only PR and s.d. responses were considered (Table 3). Tendency curves were calculated by polynomial regression. Monolayers: lower curve. Spheroids: upper curve.

As derived from Figure 7a and b, the correlation between the mitotic indexes of the original tumors and radial growth rate of the derived Sphs ($R^2 = 0.95$, plot not shown) confirmed the behavioral similarity between *in vivo* tumors and their *in vitro* models.

During our veterinary clinical study, Kg patient displayed a partial response, whereas Btl, Cl and Sc patients presented stable disease during the 5-weekly suicide gene treatments.[4] The Sc tumor had shown rapid progression *in situ* before gene therapy, with the volume increasing about five-fold in only 5 weeks (12.0–63.7 ml). Through the 5-weekly suicide gene treatment, tumor growth ceased and subsequently displayed a 38% size reduction. There was little change in size for the following 10 weeks and after that growth resumed.[4]

On the other hand, the suicide gene resistance observed in Ll and Fk tumors and derived cultures, strongly suggested re-growth resistance, even in the fast-growing monolayers. This was supported by their high mitotic index (4.5) (Table 3) and by the extremely rapid growth shown by these highly malignant amelanotic tumors *in vivo*.[4] Fk tumor had shown rapid increase in size (about 13-fold: 12.0–158.7 ml), in only 5 weeks of gene therapy, while a de-pigmenting process started. Rapid progression was also shown in Ll untreated, not easily reachable liver metastasis.[4]

Re-growth resistance to HSVtk/GCV treatment was confirmed by flow cytometry analysis

To get a deeper insight into the cellular response to HSV*tk*/GCV treatment, we checked its effects on the cell

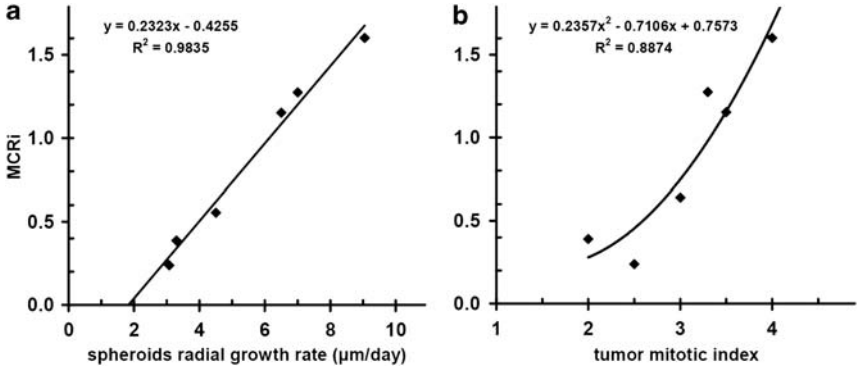

Figure 7 Correlation between the MCRi and (**a**) the radial growth rate of the tumor-derived spheroids and (**b**) the mitotic indexes of the original tumors. See Table 3. Tendency curves were calculated by linear (**a**) and polynomial (**b**) regression. Spheroids daily radial growths (μm) were determined as described in Materials and Methods: Bk, 7.0 ± 1.0; Btl, 3.0 ± 0.2; Cl, 3.3 ± 0.1; Kg, 6.5 ± 0.7; Rkb, 4.5 ± 0.4; and Sc: 9.0 ± 0.9.

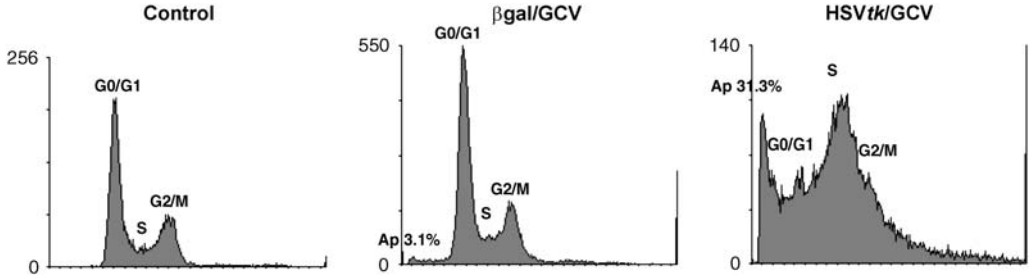

Figure 8 Flow cytometry analysis of *in vitro* untreated or βgal- and HSV*tk*-lipofected high-density Sc monolayers: Cells were grown for 48 h in the absence (control) or the presence (βgal and HSV*tk*) of 1 μg ml^{-1} GCV, suspended and treated as described in Materials and Methods. Ap, apoptosis.

cycle of high-density Sc monolayers by flow cytometry analysis (Figure 8). The mechanisms involved in cell killing confined to the outer layers of Sphs (as monolayers on the Sph surface) were similar to those of near confluent monolayers.[5,10,15]

As expected, βgal-lipofected cells were not sensitive to 1 μg ml^{-1} GCV, showing the typical cell-cycle peaks in G_0/G_1, S and G_2/M phases as in non-lipofected cells. Conversely, HSV*tk*/GCV-treated cells displayed a complex pattern where most of the cells accumulated in S and G_2/M phases, whereas about one-third of the total cells (31.3%) in the hypodiploid sub-G_1 apoptotic region displayed DNA degradation. It is noteworthy that suicide gene treatment also induced hyperploid progression, increasing the fraction of cycling, diploid and hyperdiploid cell populations actively synthesizing DNA. Then, in HSV*tk*/GCV-treated group, most of the cells continue to undergo DNA synthesis in agreement with the extremely rapid growth shown by these highly aggressive tumors in the veterinary patient. These data strongly support re-growth resistance, even in the fast-growing monolayers.

Conclusion

The development of new therapeutic strategies requires simple *in vitro* models that resemble the *in vivo* situation in order to select better treatments against solid tumors and to decrease the use of experimental animals. These models might serve as a base for a more rigorous secondary *in vitro* screening.

These data presented in this study suggest that monolayers and multicellular Sphs represent two very different experimental tumor models. Although the experiments carried out in monolayer cultures could not predict the effects of the *in vivo* treatments, the *in vitro* sensitivity of Sphs highly correlated with the clinical outcome of the HSV*tk*/GCV treatment on canine melanoma patients *in vivo* ($R^2 = 0.85$, Figure 6). This remarkable finding strongly encourages the implementation of Sphs as highly realistic experimental model for optimizing and predicting the *in vivo* response of the respective tumors to therapeutic strategies.

We found considerable response diversity to suicide gene therapy: some tumor Sphs responded well (6 of 15 displayed growth inhibition $>30\%$), whereas others showed no such response (6 of 15 displayed growth inhibition $<20\%$). *In vivo*, all the corresponding tumors presented partial response or stable disease to suicide gene therapy. Only one patient (Kg) with PR response *in vivo* generated poorly responsive Sphs. Thus, in this sample of 15 tumors, we found 47% (7/15) objective responses. Previously, we had reported 44% (7/16), 47% (21/45),[3] and 49% (25/51)[4] *in vivo* objective responses to the suicide gene system.

On the other hand, our observations suggest that opposing to the suicide gene treatment, there is an underlying Sphs MCR mechanism whose strength would be intrinsic of each individual tumor and independent of the respective monolayers response. Thus, the causes of relative MCR of tumor Sphs to therapy would be multiple: (i) the origin and type of tumor cells, (ii) their proliferation state and (iii) the heterogeneity of tumor structure.[20,21] Sphs, as experimental models to better reflect the *in vivo* tumor behavior, showed that one of the main causes of MCR would be the rapid cell repopulation (re-growth) after suicide gene treatment. The MCRi of the derived Sphs not only inversely correlated with the monolayers suicide gene sensitivity but also directly correlated with the rate of Sph growth and the mitotic index of the original tumors (Figures 5 and 7). These facts, and the highly increased fraction of HSV*tk*/GCV-treated cells actively synthesizing DNA accumulated in S and G_2/M phases as evidenced by flow cytometry analysis, strongly supported the 're-growth resistance' theory.

A highly positive message emerging from these data is the biological and clinical significance of these observations: the possible use of a new approach to evaluate the efficacy of drugs and other cancer therapies in spontaneous *in vivo* tumors. In addition to specific tumor cell marker evaluation, multicellular Sphs of each patient tumor represent a useful model (i) to find the best cancer therapies for each spontaneous *in vivo* tumor and (ii) to select patients who might benefit from a specific therapy. All this provides the rationale for future controlled therapy trials of multicellular Sphs of each patient tumor-directed therapy versus physician's choice to determine whether assay-directed treatment can improve the patient's response and survival.

Materials and methods

Cell cultures

Cultured cells derived from surgically excised canine melanomas were obtained by enzymatic digestion of tumor fragments with 0.01% Pronase (Sigma, St. Louis, MO, USA) and 0.035% DNase (Sigma) or by mechanical disruption in serum-free culture medium.[10,11] They were cultured as monolayers and multicellular Sphs at 37 °C in a humidified atmosphere of 95% O_2/5% CO_2 with Dulbecco's modified Eagle's medium/F12 medium (Invitrogen, Carlsbad, CA, USA) containing 10% fetal bovine serum (Invitrogen), 10 mM HEPES (4-(2-hydroxyethyl)-1-piperazineethanesulfonic acid) (pH 7.4) and antibiotics. Serial passages were done by trypsinization (0.25% trypsin and 0.02% EDTA in phosphate-buffered saline) of sub-confluent monolayers.

Immunocytochemistry

Cells attached onto a glass slide were cultured for 48 h in the above-described conditions. Then, the cells were washed, fixed with cold acetone, dried, re-hydrated and incubated separately with the following specific monoclonal antibodies as described by the manufacturers: anti-human melan A (BioGenex, San Ramon CA, USA; clone A103), anti-human S-100 (BioGenex; clone 15E2E2), anti-human GP100 (BioGenex; clone HMB45) anti-human vimentin (Dako, Glostrup, Denmark; clone V9); anti-human cytokeratin (Dako; clones AE1/AE3). After washing, cells were incubated with Multi-Link immunoglobulins (BioGenex) followed by streptavidin/peroxidase conjugate and developed with 3,3′-diaminobenzidine.

Plasmids

Plasmid psCMVβ was built by replacing the HSV thymidine kinase gene of psCMV*tk* [10] by *Escherichia coli* β-galactosidase gene from pCMVβ.[12] Plasmids were amplified in *E. coli* DH5α (Invitrogen), grown in LB medium containing 100 μg ml^{-1} neomycin and purified

by ion-exchange chromatography (Qiagen, Valencia, CA, USA).

Liposome preparation and in vitro *lipofection*

DC-Chol (3β*N*-(*N*′,*N*′-dimethylaminoethane)-carbamoyl cholesterol) and DMRIE (1,2-dimyristyloxypropyl-3-dimethyl-hydroxyethilammonium bromide) were synthesized and kindly provided by BioSidus (Buenos Aires, Argentina). DOPE (1,2-dioleoyl-*sn*-glycero-3-phosphatidyl ethanolamine) was purchased from Sigma. Liposomes were prepared at lipid/co-lipid molar ratios of 3:2 (DC-Chol/DOPE) or of 1:1 (DMRIE/DOPE) by sonication as described.[13,14] Optimal lipid mixtures were determined for every cell line.[10]

Cultured cells at a density of 5×10^4 cells per cm^2 (about 40% confluence) were exposed to lipoplexes (1 μl liposomes per cm^2 and 0.5 μg DNA per cm^2) during 4–6 h.[10]

β-Galactosidase staining

To measure gene transfer efficiency, psCMVβ-lipofected cells were trypsinized, fixed in suspension, stained with 5-bromo-4-chloro-3-indolyl β-D-galactopyranoside (X-GAL, Sigma) and counted using an inverted phase contrast microscope.[10]

Sensitivity to GCV assay

At 24 h after lipofection, both transiently HSV*tk*- and βgal-expressing cells, were seeded on regular plates as monolayers ($3.5–7.0 \times 10^4$ cells per ml) or on top of 1.5% solidified agar to form Sphs (2.0×10^5 cells per ml) and incubated with medium containing from 0.01 to 1000 μg ml^{-1} GCV (synthesized and kindly provided by BioSidus). After 5 days in monolayers or 12 days in Sphs, cell viability was quantified using a colorimetric CellTiter 96 Aqueous Non-Radioactive MTS Cell Proliferation Assay according to the manufacturer's instructions (Promega, Madison, WI, USA). The percentage of cell survival was calculated from the ratio of the absorbances between cells incubated in the presence or absence of GCV.[10] The cell sensitivity to GCV, expressed as the prodrug concentration that inhibited cell survival by 50% (IC_{50}), was estimated from dose–response curves.

Sphs growth

The size of sparse growing MCS was estimated during a period of 15 days using a Neubauer chamber (Thomas Scientific, Swedesboro, NJ, USA) under an inverted microscope.[10,15] The average diameter of MCS was recorded as measure of two diameters. Results were expressed as mean (of a minimum of 15 Sphs diameters) ± s.e.m. (n = four independent assays).

Flow cytometry cell-cycle analysis

Untreated cells or both HSV*tk*- and βgal-expressing cells in culture in the presence of 1 μg ml^{-1} GCV for 48 h were trypsinized, fixed in 70% (v/v) ethanol at −20 °C for 1 h, treated with RNase, stained with 10 μg ml^{-1} propidium iodide for 30 min and subjected to single-channel flow cytometry on a Becton Dickinson FACScan (Franklin Lakes, NJ, USA), with collection and analysis of data performed using Becton Dickinson CELLQuest software.[5]

Patients

Dogs with a confirmed histopathological diagnostic of melanoma were recruited for a study as it was reported.[3,4] The dogs' owners were notified about the experimental nature of the treatment, and all of them granted written informed consent for treatment.[3,4] The treatment was performed by specially trained veterinary professionals, working in accordance with the laws and regulations of our country (Argentina). All scientific and ethical issues related to the veterinary clinical trial were evaluated and approved by the appropriate committee of the granting agency (ANPCYT, Argentina).

Treatment

The patients selected for this study displayed local disease (partially removed tumor, or postsurgical relapse) and received multiple injections of lipoplexes carrying psCMV*tk* (1–4 mg DNA) co-delivered with GCV (5–20 mg) in the remaining tumor or adjacent areas, according to tumor size. At 24 and 48 h after SG plus GCV delivery, patients orally took 400–800 mg of acyclovir according to their weight. They continued with a weekly local treatment chronically or until disappearance of any evidence of local disease.[4] In addition, between 5 and 10 days after surgery, patients were clinically controlled and treated once a week for 5 weeks with a subcutaneous vaccine composed of autologous and/or allogeneic formalized tumor cells and irradiated living CHO xenogeneic cells producing 20–30 mg of hIL-2 and hGM-CSF.[4] Tumor volumes were calculated as $4/3 \times \pi \times r_1 \times r_2 \times r_3$.[4]

Statistics

Results were expressed as mean ± s.e.m. (n: number of experiments corresponding to independent assays). Differences between groups were determined by analysis of variance (ANOVA).

Conflict of interest

The authors declare no conflict of interest.

Acknowledgements

We thank Graciela Zenobi for technical assistance, Lina Marino for expert immunocytochemical analysis and María D Riveros and Dr Armando L Karara for their contribution in the early stages of this study. This study was partially supported by a grant from ANPCYT-FONCYT: BID1728/OC-AR—PICT 2002—12084 and PID-UBACYT-2008/2010—M027. G.C.G. and L.M.E.F. are investigators, and M.L.G.C. and M.S.V. are fellows of the Consejo Nacional de Investigaciones Científicas y Técnicas (CONICET, Argentina).

References

1 Ramos-Vara JA, Beissenherz ME, Miller MA, Johnson GC, Pace LW, Fard A *et al*. Retrospective study of 338 canine oral melanomas with clinical, histologic, and immunohistochemical review of 129 cases. *Vet Pathol* 2000; **37**: 597–608.
2 Smith SH, Goldschmidt MH, McManus PM. A comparative review of melanocytic neoplasms. *Vet Pathol* 2002; **39**: 651–678.

3 Finocchiaro LME, Fiszman GL, Karara AL, Glikin GC. Suicide gene and cytokines combined non viral gene therapy for canine spontaneous melanoma. *Cancer Gene Ther* 2008; **15**: 165–172.
4 Finocchiaro LME, Glikin GC. Cytokine-enhanced vaccine and suicide gene therapy as surgery adjuvant treatments for spontaneous canine melanoma. *Gene Therapy* 2008; **15**: 267–276.
5 Altamirano NA, Karara AL, Villaverde MS, Fiszman GL, Glikin GC, Finocchiaro LME (2007). Spontaneous canine melanoma derived spheroids display individual multicellular resistance patterns to suicide gene and chemotherapy. In: Torres LS (ed). *Cancer Drug Resistance Research Perspectives*. Nova Science Publishers, Inc.: New York., pp 119–137, ISBN: 1-60021-572-6.
6 Mesnil M, Yamasaki H. Bystander effect in herpes simplex virus-thymidine kinase/ganciclovir cancer gene therapy: role of gap-junctional intercellular communication. *Cancer Res* 2000; **60**: 3989–3999.
7 Desoize B, Jardillier JC. Multicellular resistance: a paradigm for clinical resistance? *Crit Rev Oncol Hematol* 2000; **36**: 193–207.
8 Santini MT, Rainaldi G. Three-dimensional spheroid model in tumor biology. *Pathobiology* 1999; **67**: 148–157.
9 Sutherland RM. Cell and environment interactions in tumor microregions: the multicell spheroid model. *Science* 1998; **240**: 177–184.
10 Finocchiaro LME, Bumaschny VF, Karara AL, Fiszman GL, Casais CC, Glikin GC. Herpes simplex virus thymidine kinase/ganciclovir system in multicellular tumor spheroids. *Cancer Gene Ther* 2004; **11**: 333–345.
11 Karara AL, Bumaschny VF, Fiszman GL, Casais CC, Glikin GC, Finocchiaro LM. Lipofection of early passages of cell cultures derived from murine adenocarcinomas: *in vitro* and *ex vivo* testing of the thymidine kinase/ganciclovir system. *Cancer Gene Ther* 2002; **8**: 96–99.
12 MacGregor GR, Caskey T. Construction of plasmids that express *E coli* β-galactosidase in mammalian cells. *Nucleic Acids Res* 1989; **17**: 2365–2365.
13 Felgner JH, Kumar R, Sridhar CN, Wheeler CJ, Tsai YJ, Border R *et al*. Enhanced gene delivery and mechanism studies with a novel series of cationic lipid formulations. *J Biol Chem* 1994; **269**: 2550–2561.
14 Gao X, Huang L. Cationic liposome-mediated gene transfer. *Gene Therapy* 1995; **2**: 710–722.
15 Casais CC, Karara AL, Glikin GC, Finocchiaro LME. Effects of spatial configuration on tumor cells transgene expression. *Gene Ther Mol Biol* 2006; **10**: 207–222.
16 Inoue K, Ohashi E, Kadosawa T, Hong SH, Matsunaga S, Mochizuki M *et al*. Establishment and characterization of four canine melanoma cell lines. *J Vet Med Sci* 2004; **66**: 1437–1440.
17 Hendrix MJ, Seftor EA, Chu YW, Seftor RE, Nagle RB, McDaniel KM *et al*. Coexpression of vimentin and keratins by human melanoma tumor cells: correlation with invasive and metastatic potential. *J Natl Cancer Inst* 1992; **84**: 165–174.
18 Koenig A, Wojcieszyn J, Weeks BR, Modiano JF. Expression of S100a, vimentin, NSE, and melan A/MART-1 in seven canine melanoma cells lines and twenty-nine retrospective cases of canine melanoma. *Vet Pathol* 2001; **38**: 427–435.
19 Mueller-Klieser W. Tumor biology experimental therapeutics. *Critical Rev Oncol Hematol* 2000; **36**: 123–139.
20 Brown JM, Giaccia AJ. The unique physiology of solid tumors: opportunities (and problems) for cancer therapy. *Cancer Res* 1998; **58**: 1408–1416.
21 Siemann DW. The tumor microenvironment: a double-edged sword. *Int J Radiat Oncol Biol Phys* 1998; **42**: 697–699.
22 Spangler WL, Kass PH. The histologic and epidemiologic bases for prognostic considerations in canine melanocytic neoplasia. *Vet Pathol* 2006; **43**: 136–149.